A review of the regional maximum flood and rational formula using geomorphological information and observed floods

Geoff Pegram* and Mohamed Parak
Civil Engineering Programme, University of KwaZulu-Natal, Durban 4041, South Africa

Abstract

Flood estimation methods in South Africa are based on three general approaches: empirical, deterministic and probabilistic. The "quick" methods often used as checks are the regional maximum flood (RMF) and the rational formula (RF), which form part of the empirical and deterministic methods respectively. A database of annual flood peaks was used in a probabilistic approach to review these methods and to provide preliminary insight into their estimates of flood peaks. This paper examines the following: the relationship between floods and landscape; the estimation of the return period of the RMF; the use of ratios in scaling RMF flood peak estimates to flow rates of shorter return periods; the applicability of the modified rational formula (MRF); the examination of the relationship between scaling parameters and regional parameters. It turns out that the RMF is the best of all methods examined in this preliminary study (other than statistical) in estimating the 200-year flood peak at an ungauged location.

Keywords:flood estimation, rational formula, regional maximum flood, generalised extreme value distribution

Introduction

The realistic estimation of the magnitude of a design flood peak with a chosen probability of exceedence that can be expected at a given site in a given region is fundamentally important in the planning, design and operation of hydraulic structures and for the preservation of human life and property. The basic approaches involved in flood estimation are the empirical, deterministic and probabilistic approaches. These methods are calibrated from historical flood records from gauged catchments and their relative usefulness depends on the accuracy with which they are able to predict flood sizes in ungauged catchments. In South Africa, reasonable estimates of maximum recorded flood magnitudes are derived from the use of the empirically-based approach of the regional maximum flood (Kovacs, 1988), and design floods may be determined using deterministic approachs such as the rational formula (RF), the SCS model or the unitgraph method and from the analyses of flood frequencies through a probabilistic approach.

Kovacs' **empirical method** is probably the most robust method available locally and, relatively accurately, predicts the regional "maximum" flood that can be expected from a given site based only on the site's catchment area and region. The advantage of the empirical method is its ease of use as it deals directly with the parameter of interest, namely the flood peak discharge, and avoids the assumptions involved in transforming rainfall inputs into flood outputs. The disadvantages of the RMF method are that:

- The recurrence interval (RI) associated with this "maximum" is not clear, although Kovacs estimated it to be greater than 200 years
- The regions defined by individual *K*-values have widely varying rainfall properties and
- It seems naive to estimate flood peaks on area and zone only.

* To whom all correspondence should be addressed.
☎+2731 260-3057; fax:+2731 260-1411; e-mail: pegram@ukzn.ac.za
Received 8 January 2004; accepted in revised form 14 May 2004.

The **deterministic** rational formula (RF) approach involves (in a simple, but sound manner) the analysis of all the factors involved in flood prediction from converting rainfall inputs into flood outputs; it usually carries a caveat that it should not be used for "large" catchments, but recent work (Alexander, 2002 and Pegram, 2003) has shown that this caution is too conservative.

Flood **frequency analysis** involves the fitting of a probability model to the sample of annual flood peaks, recorded over a period of observation, for a catchment of a given region. The model parameters established can then be used to predict the extreme events of large recurrence interval. The advantage of this method is that the events of large recurrence interval, which are longer than the record period, can be determined through cautious extrapolation of the fitted distribution based on the model parameters. The disadvantage of this method is that it can only be applied where data have been collected and it is often not clear how the analysis can be extended to ungauged locations.

The question that arises is "which method is fair to use?" The answer depends on the availability of data. When no hydrological (rainfall and runoff) records exist for a catchment, the empirical methods provide the only means of flood prediction. This situation is the most common case in the design of hydrological projects. When estimates of design rainfall are available (Adamson, 1981; Smithers and Schulze, 2003) or rainfall records suitable for a frequency analysis are available from a nearby rain-guage, then the rational formula (RF) becomes applicable, in addition to the empirical. When flood records of sufficient length (>30 years or so) exist, possible future flood peaks of given frequency can be determined by modelling past floods with an extreme value distribution. Even in this fortunate situation, it is prudent to crosscheck the frequency estimate with deterministic and empirical estimates.

It is the aim of this exploratory study to provide a review of the above methods in order to determine the accuracy of the estimates of the design flood, where the design flood is the flood associated with a chosen return period or recurrence interval of exeedence. The base data are the set of annual flood peak records from 130 sites around South Africa that were used *inter alia* by Kovacs (1988) in his empirical study.

To summarise: this paper attempts to provide preliminary insight into the following questions concerning the RMF and RF flood determination methods in South Africa using the recorded flood peaks:

- Does the addition of landscape data (catchment morphometry) improve the prediction of floods by the RMF?
- Can a return period be associated with the RMF by comparing its computed magnitude with those modelled from historical records?
- Are simple country-wide Q_T/Q_2 ratios valid for scaling flood maxima (or RMF values) to floods of shorter (or even longer) return periods?
- Is the modified rational formula (MRF) a useful modification and reasonable alternative to the RF and other flood prediction methods?
- Are there any inferences that can be drawn from the variation of the shape parameters *k* of the GEV Distribution, used to model the observed floods, and Kovacs' regional *K*-values?

The methodologies involved in assessing each of the objectives listed in this paper will be expanded in detail in the sequel. Before this can be done, an explanation of how the recorded data set was used in the calibration and validation of the objectives outlined is given.

The use of recorded flood data in this study

Annual flood peaks from 130 catchments across South Africa were obtained from Zoltan Kovacs of the Department of Water Affairs by Peter Adamson while working with the first author in 1988 and 1989. This data set, although old (final year of record was 1988), provided the starting point for this pilot study in the review of these flood determination methods. The length of record of the data set used herein ranged from 9 years to 76 years and forms a sub-set of the data used by Kovacs for the construction of the RMF curves. To find the return period associated with each annual peak, the Weibull Plotting Position was used (it is more conservative than the Cunnane Plotting Position), which is expressed as:

$$T = \frac{N+1}{r} \quad (1)$$

where:

T is the return period (years) associated with the flood peak of rank *r*
N is the length of record (years)
r is the rank of the flood peak; r = 1 for the largest peak.

This resulted in a list of annual peaks each with an associated return period for each catchment. Following the work of De Michele and Salvadori (2002) and Kjeldsen et al. (2002), the distribution of these peaks was assumed to follow a generalised extreme value (GEV) distribution. This distribution takes the following form:

$$Q_T = \mu + \sigma y_T \quad (2)$$

where:

Q_T is the *T-year* return period flood peak estimate
μ, σ are shift and scaling parameters respectively
y_T is the GEV reduced variate corresponding to a *T*-year return period, i.e.

$$y_T = \frac{1}{k}\left[1-\left\{-\ln\left(1-\frac{1}{T}\right)\right\}^k\right] \quad (3)$$

where:

k is a shape parameter. When k = 0, the GEV reduces to the EV1 or Gumbel distribution.

This model of the flood data formed the basis with which to review the other approaches. Some of these data and their distribution fits are presented in Table A1 (Part 3) in the **Appendix**.

Empirical approach extended by including landscape properties

In his empirical approach Kovacs (1988) determined envelopes of the maximum flood peaks from the original extended data set, of which, as has been noted above, the data in the **Appendix** are a subset. Kovacs' data set included some rare singleton floods (not used in this study) to which he cautiously ascribed a representative record length not exceeding 200 years. He used this extended set to obtain the RMF lines based on the Francou-Rodier equation. The technique was to plot maximum flood peaks against catchment area for hydrologically homogeneous regions to produce envelope curves which define the upper limit of expected flood peaks for a given region. The curves are defined by the following equation:

$$Q_{RMF} = 10^6\left(\frac{A}{10^8}\right)^{1-0.1K} \quad (4)$$

where:

A is catchment area in km^2
K is a regional dimensionless factor which accounts for the influence of variations in rainfall, geology, land-form and vegetation cover in flood production.

It should be noted at this juncture, that the "secret" to the success of the RMF is the careful way in which Kovacs chose the regions to group the flood data. He did this by examining the actual *K*-value (from Eq. (4)) for each catchment where the flood peaks and catchment areas were known. Regional boundaries of *K* were delimited by considerations of individual *K*-values within the region, the number and accuracy of the data in a particular area, existing boundaries, maximum recorded 3 day storm rainfall, topography, catchment orientation with respect to dominant storm generating weather systems, general soil permeability, main drainage network and the location of large dams situated upstream from the guaging sites (Kovacs, 1988). Of these considerations, individual *K*-values were evidently the most important and the regions were traced based on this. In areas of high flood peak potential a difference of 0.2 between individual *K*-values was allowed for and a difference of 0.6 in areas of low flood peak potential.

What is evident from Eq. (4), and all other derived empirical equations produced for the prediction of floods, is its dependence on *Area* as an independent variable. Because of the RMF's apparent naivety, one might expect other parameters of the fluvial landscape to play an important role in flood response and make the estimates more accurate. Flood geomorphologists, such as Horton (1932; 1945) and Strahler (1952; 1964) and many others since have been interested in relating flood discharges to physical measures of landscape (morphometry). They identified parameters of the fluvial landscape which intuitively would correlate well with flood discharge.

Linear parameters (such as stream orders and stream lengths), areal parameters (such as catchment area, catchment shape and drainage density) and relief parameters (such as catchment relief, catchment slope, channel slope and ruggedness number) are some of the physical measures that have been identified as significantly

affecting flood response. One can expect such a relationship between flood discharge and catchment morphometry to exist because a catchment is effectively "an open system trying to achieve a state of equilibrium" (Strahler, 1964). Precipitation is input to the system and soil (eroded material) and excess precipitation leave the system through the catchment outlet. Within this system an energy transformation takes place converting potential energy of elevation into kinetic energy where erosion and transportation processes result in the formation of topographic characteristics. Thus it is evident that floods, and the landscape through which they drain, form a mutual relationship and ultimately catchment morphometry should reflect this phenomenon. In this pilot study, an effort is made to determine if landscape parameters improve the prediction of floods in empirical equations based solely on catchment area.

TABLE 1
Ratio between T-year flood and 2-year flood (TRH 25, 1994)

T	2	10	20	50	100	200	1000	10000
$\mathbf{Q_T/Q_2}$	1	3.57	5.18	7.80	10.24	13.14	22.00	41.24

What is the recurrence interval of the RMF?

What is also evident from the RMF method of flood determination is that one is not easily able to associate a return period with the estimated floods. The envelope floods (estimated from the RMF lines) have been described as the maximum flood that the site has experienced. This is not easy to quantify in terms of a return period. Kovacs himself estimates the return period to be greater than 200 years (Kovacs, 1988), although he does not explicitly model their probability distribution. Where the representative period (N) of a flood was not known, Kovacs did not allow this to exceed 200 years and a provisional N value was estimated based on the assumption that the ratio of the 200-year peak to RMF, Q_{200}/RMF was 0.65.

When determining a design flood, the exact magnitude of the flood and its probability of exceedance need to be known. The absence of an estimate of the return period associated with the RMF makes the quantification of risk by this method problematic and, as it represents maximum discharges, it tends to be used by designers as a conservative method. This article aims to, *inter alia*, determine a return period associated with the RMF by simultaneously plotting the floods determined from the RMF method and the historical floods extrapolated to the 50-, 100- and 200-year recurrence intervals modelled with the GEV distribution.

The first author has for many years suggested that the RMF envelopes have a recurrence interval of about 200 years, as estimated by the Weibull Plotting Position. This estimate was based on the following argument: the data used by Kovacs (1988) in the construction of the RMF lines had, in many instances, record lengths (actual and estimated) of the order of 100+ years. The RMF lines are envelopes, drawn above the data whose maximum record length N was 200 years. If we are conservative and estimate the recurrence interval of the RMF line using the Weibull Plotting Position, the RI (T) of the largest observation would be $T_N = (N+1) \approx 200$ *years*. It was decided to examine this conjecture as part of this study.

The use of Q_T/Q_2 ratios for scaling flood maxima

It is useful to know how to scale the "200-year RI" RMF or any other flood of recurence interval T-years to shorter return period floods where desired. The first author suggested such a scaling in Chapter 2 of TRH 25 (1994). It was thought that this study was also an opportune time to check that assumption which was based on the following argument.

Hiemstra and Francis (1979) examined the relationship between the peak flood discharge of a catchment and its hydrograph shape defined by the volume. What they discovered was that for extreme events, the peak discharges of various magnitudes were well modelled by the censored log-normal distribution. They extracted the statistics of many floods in the Department of Water Affairs and Forestry's break-point continuous flow rate database at that time and found the coefficient of variation of the peak discharges averaged 1.3 with a fairly small variation. Based on this, the first author produced ratios which relate the T-year flood to the 2-year flood. These ratios, Q_T/Q_2 reproduced from TRH 25 (1994) in Table 1, enable one to convert any flood of a given RI to a T-year flood.

To check this assumption in this study, the maximum observed flood recorded in the observation period from each of the 130 catchments was associated with a return period using the Weibull Plotting Position ($T_{max} = N+1$). This flood was then scaled to 10- and 50-year flow rates using the Q_T/Q_2 ratios and compared with those computed from the GEV model fitted to the full set of data in each record. These values were then compared and it was determined if these ratios are applicable in reducing flood maxima to floods of desired recurrence intervals.

The modified rational formula (MRF)

The ratonal formula is expressed (in *SI* units) as:

$$Q_{peak} = ciA/3.6 \qquad (5)$$

where:

- c is a dimensionless runoff coefficient which ranges from 0 to 1
- i is the intensity of rainfall (mm per hour) of return period T (years) and duration T_c, where T_c is the time of concentration (hours) of the catchment
- A is the area of the catchment (in km^2).

This formula is usually limited to catchments with small areas (< 100 km^2). The reason usually given for this is that the formula does not take into account the areal reduction factor (*ARF*) and utilises point design rainfall intensity. It should be noted that flood-causing rainfall in smaller catchments is mainly due to concentrated thunderstorm activity, whereas flood-producing rainfall in larger catchments is mainly due to long-duration, widespread synoptic events (Pegram, 2003). The consequence is that the larger the catchment, the longer the duration of the flood-causing rainfall. To simplify the analysis, Pegram (2003) used the scaling properties of the GEV distribution fitted to rainfall depths, hence, using the GEV distribution defined in Eq. (3), the precipitation scaling relationship becomes:

$$P_{d,T} = (\mu + (\sigma/k)[1-\{-\ln(1-1/T)\}^k])d^{1-\eta} \qquad (6)$$

where:

$P_{d,T}$ is the rainfall depth of duration d and return period T.

For each of Kovacs' regions, representative 1-, 2- and 3-day rainfall depths for 2-, 5-, 10-, 20- and 50-year return periods were extracted

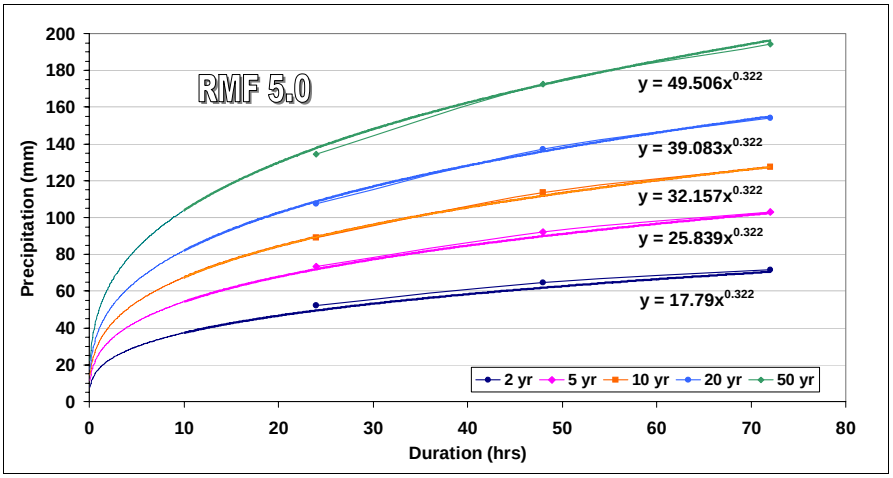

Figure 1
Fit based on the GEV (smooth curves), to an average of Adamson's (1981) data (dots) for Kovacs (1988) RMF Region 5 (from Pegram, 2003). The thin lines are trend-lines fitted to each set of the 1-, 2- and 3-day rainfall duration data. The thick lines are the combined models fitted to all the data with a common power law relationship.

from Adamson (1981) by Westray (2001). These were averaged (pooled) by region and Eq. (6) was fitted to the 15 points by Least Squares. An example is given in Fig. 1 where the pooled data and the fitted function are compared for Region 5. The k and η values were fixed at -0.182 and 0.678 respectively by using the whole South African data set as a first approximation (Pegram, 2003). Values of μ and σ were the parameters that were estimated for each region. It was found that the coefficient of variation $C_v = \sigma/\mu$ was effectively independent of Kovacs' regions, so the major variable to concentrate on was the parameter μ.

In addition to this simplification, for all the catchments whose data are available in the report by Petras and Du Plessis (1987), the time of concentration T_c computed from the Kirpich (1940) formula: $T_c = 0.0633(L/S)^{0.385}$ (where as usual, L is the length and S is the average slope of the catchment's longest watercourse) was set to the duration of the flood-causing storm as demanded by the RF. When this duration T_c was plotted against area, the points clustered around a curve to which a power law relationship could be fitted. This is also the practice in Australian Rainfall and Runoff (AR&R, 2001). For interest sake, this was superimposed on the areal reduction factor (ARF) diagram, published in the Flood Studies Report (FSR, 1975), which appears as Fig. 2. It is possible that the FSR's ARF curves over-estimate the ARF in South Africa, but the degree is likely to be a matter of climate. Conscious of this, it is still remarkable that the *Area* ~ T_c curve yields an almost constant ARF value of 88% across the FSR curve. Thus, as long as the precipitation intensity used in the rational formula corresponds to the time of concentration of the catchment, the point rainfall is automatically scaled by a constant ARF. Combining these ideas, the MRF was then expressed (Pegram, 2003) in preliminary form as:

$$Q_{MRF} = c \times 0.318 P_{1day,2} \left[1 + 0.385 y_T\right] A^{0.558} \qquad (7)$$

where:

- c is the conventional rational formula (RF) c: $0 < c < 1$
- $P_{1day,2}$ is the median 1d annual maximum rainfall available from maps (e.g. Adamson, 1981; Smithers and Schulze, 2003)
- y_T is the reduced variate of the GEV Distribution of the rainfall
- A is the catchment area in km^2.

In this paper the 10-, 20- and 50-year floods of the MRF are compared with the observed flood peaks modelled with the GEV distribution of the same recurrence intervals. The intention is to determine whether the MRF in its coarse form is possibly a useful candidate for predicting the design floods of a catchment.

Does the GEV regionalise following the RMF?

The annual observed flood data series, extracted from the observed records, were modelled using the GEV distribution. This was explained above. The records were thought to be long enough, in most cases, to make reasonable predictions of future events. Following this analysis, it was of interest to determine if the shape parameter k established by modelling historical floods using the GEV distribution, display any trends with a region descriptor such as Kovacs' regional K-value. That concludes the introduction. The full analyses are reported in the following sections.

Floods and landscape

Landscape data from 25 catchments were extracted in a preliminary study by Parak (2003) that corresponded with the peak discharges of the catchments modelled in this study. Parak (2003) captured morphometric data of 45 catchments across the country in his investigation into the relationship between floods and landscape. He used already catalogued data (Petras and Du Plessis, 1987 and Kovacs, 1988) and supplemented this with further data through map work from Midgley et al. (1994). In this paper the landscape data were utilised to assess whether they improved the prediction of floods compared with the RMF, which uses only catchment areas in particular regions. The flow rate that was used for comparison here was the 20-year event determined by modelling the historical floods of the catchments using the GEV distribution, the rationale being that:

- It would be the least likely estimate to be affected by fitting the wrong probability distribution
- Many of the records were longer than 20 years.

The flood and landscape data were split into two groups, one for calibration and the other for validation. The landscape data included catchment area, mean channel slope, mean annual precipitation, drainage density, catchment relief and ruggedness number. These are summarised in Table A1 and explained in the **Appendix** and a typical catchment and its derived geometry are shown in Fig. 3 (from Parak, 2003). It is aknowledged that the landscape data catalogued are sensitive to map scale, i.e. at different scales, different values of the parameters will be obtained. For example, the river detail shown on a larger scaled map is much less than that which is shown on fine-scaled maps. This has a direct influence on the magnitudes of the landscape parameters. Measures such as total stream length, stream orders, drainage densities and ruggedness

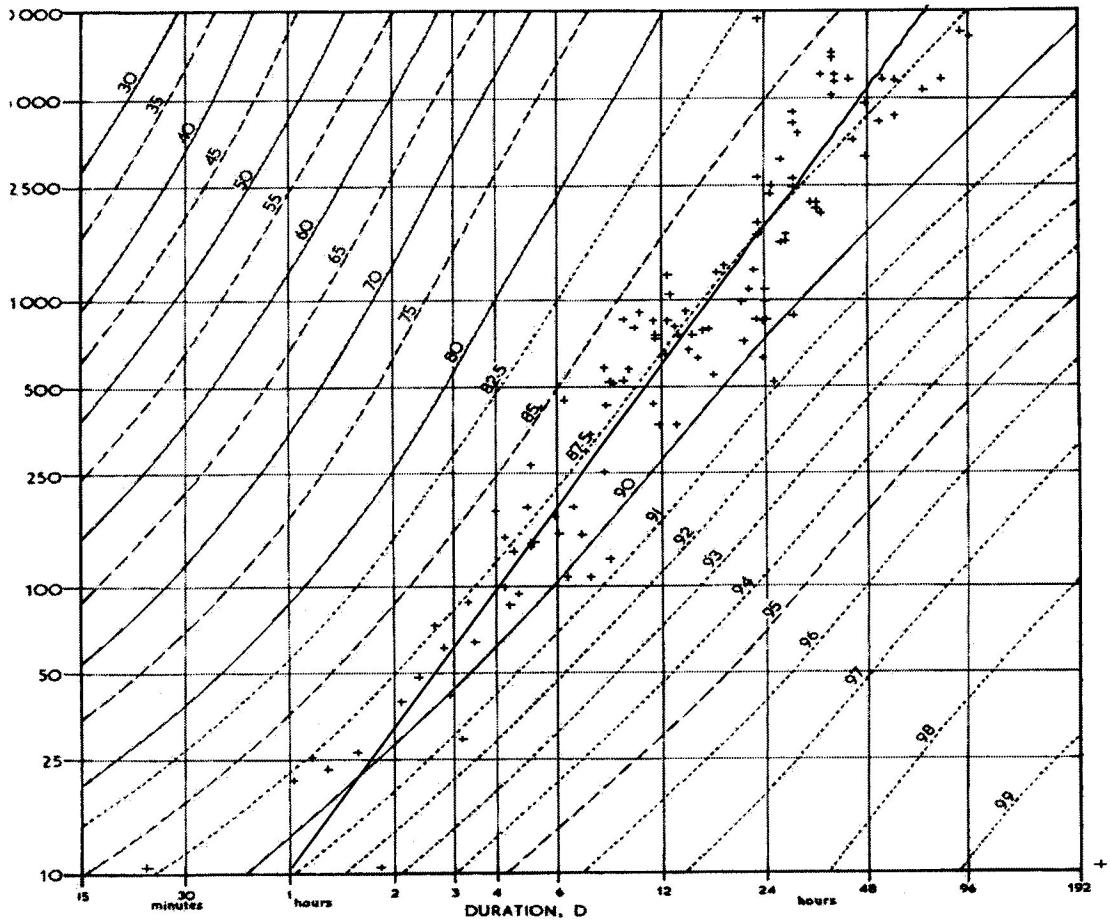

Figure 2
The FSR diagram for ARF (FSR, 1975), as contours in percentages, with T_c vs area relationships (using Kirpich's (1940) formula: $T_c = 0.0633 (L/S)^{0.385}$) for South African catchments superimposed (Westray, 2001). The best fit is: $T_c = 0.148 A^{0.651}$.

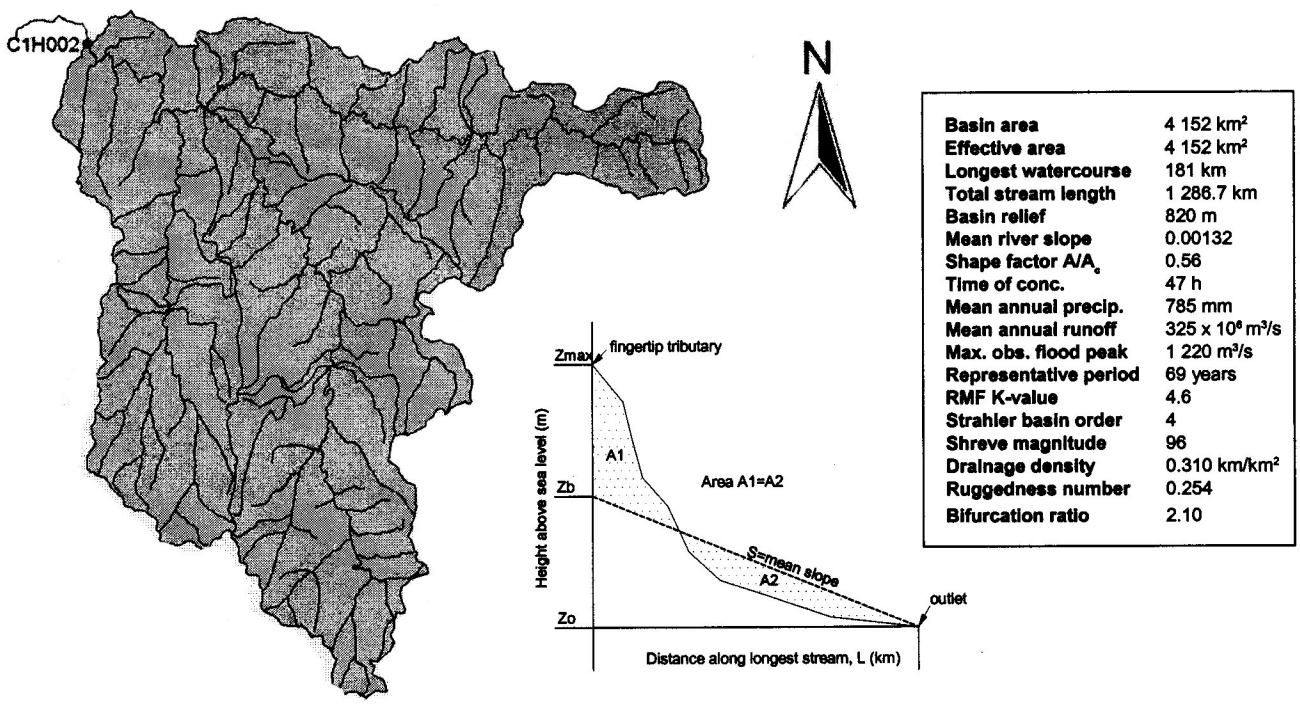

Basin area	4 152 km²
Effective area	4 152 km²
Longest watercourse	181 km
Total stream length	1 286.7 km
Basin relief	820 m
Mean river slope	0.00132
Shape factor A/A_c	0.56
Time of conc.	47 h
Mean annual precip.	785 mm
Mean annual runoff	325 x 10^6 m³/s
Max. obs. flood peak	1 220 m³/s
Representative period	69 years
RMF K-value	4.6
Strahler basin order	4
Shreve magnitude	96
Drainage density	0.310 km/km²
Ruggedness number	0.254
Bifurcation ratio	2.10

Figure 3
Plan, long section and basin properties of the Klip River catchment (represented by gauge C1H002) in the eastern highveld area of South Africa (Petras and Du Plessis, 1987; Kovacs, 1988; Midgley et al., 1990 and Parak, 2003). Reference should be made to the ***Appendix*** *for the definitions of these parameters and those summarised in Table A1.*

numbers are all dependent on the scale of the map from which these parameters were extracted. More accurate measures can be made with the use of finer scaled maps, but this comes at the expense of greater effort and time requirements. Parak (2003) used uniform scaled maps from Midgley et al. (1990) showing river detail at 1:250 000 for the data extraction.

The criterion for choosing an appropriate model was based on the determination of the R^2 statistics through stepwise regressions. The first group of flow rates were plotted against catchment area to determine a regression equation and R^2 statistic in the calibration set. The regression equation was then used to generate flow rates of the second (validation) group from the independent variable and these estimates were plotted against the recorded ones of the same group to see if they mimicked each other. The degree of validation was based on the strength of the R^2 statistic. Subsequently, other landscape data were combined with catchment area to examine if they improved the strength of the relationship (based on the R^2 statistic) in calibration and validation. A conclusion was drawn based on the examination of the R^2 statistic in calibration and validation of the two groups of flood and landscape data.

In the original study Parak (2003) examined the relationship between the flood peaks and the various candidate landscape parameters. The model, given by Eq. (8), was selected after examining the literature on geomorphological estimates of floods and carefully plotting pairs of variables. A power-law relationship was selected and various groupings of "independent" variables were included in the regression equation, which was the logarithm of Eq. (8), shown as Eq. (9). The model selection process was performed by fitting the model to a calibration set and checking the fit for a validation set. The most suitable formulation was a power relationship of the form:

$$Q_{20} = aA^bX^cY^d.... \quad (8)$$

where:

a, b, c and d are parameters to be regressed from the data and A, X and Y are landscape quantities.

The formulation for regression was to take logarithms of Eq. (8) and regress using the linearised model:

$$\log(Q_{20}) = \log(a) + b.\log(A) + c.\log(X) + d.\log(Y) \quad (9)$$

Figure 4 shows the calibration of the empirical equation defining the 20-year flood as a function of catchment area. The R^2 statistic from this model implies a strong relationship (0.856) and good fit. When this empirical model is tested against the reserved data of the second group in validation (Fig. 5), the fit is evidently poor, producing a moderate R^2 statistic of 0.538. When further landscape data are added to catchment area in the hope of improving the fit of the empirical models, the results are no better. The addition of landscape data as independent variables in the prediction of floods did not improve flood prediction and it seemed as though the best model of floods and landscape is simply area based. These results

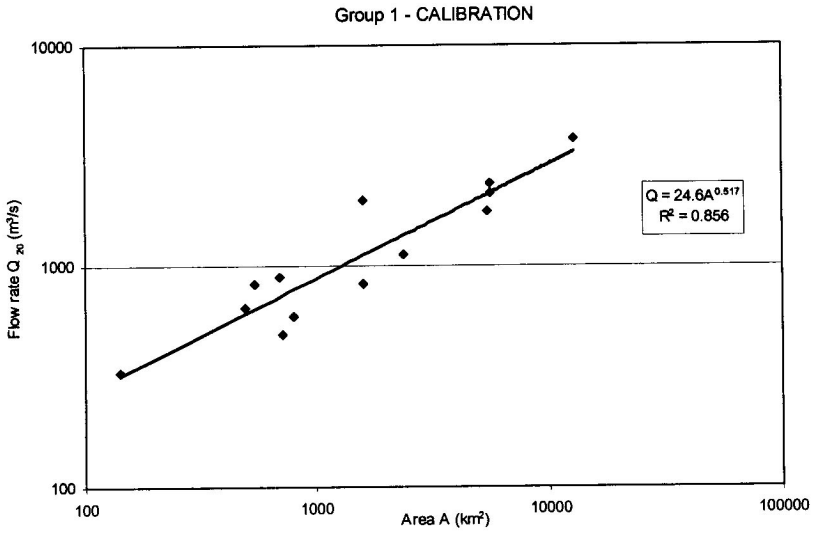

Figure 4
Q_{20} vs. area - calibration set for 13 catchments

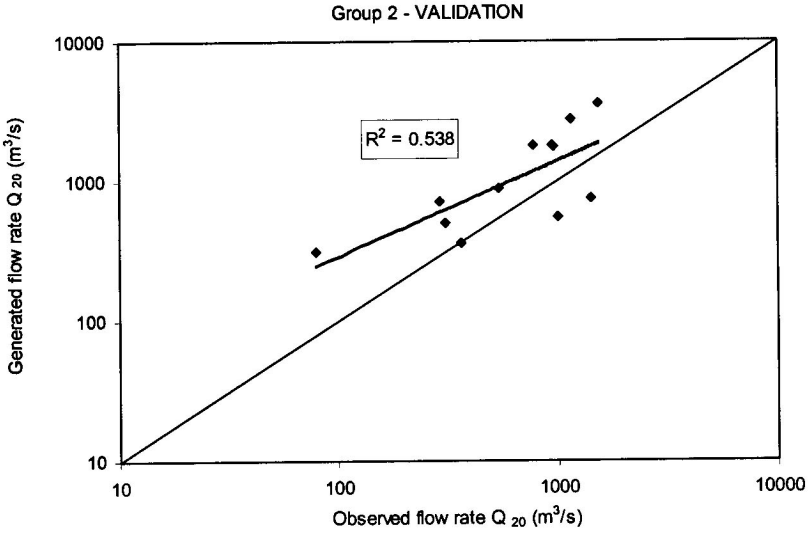

Figure 5
Generated flow rates (based on the regression of Fig. 4) vs. observed flow rates for the 20-year return period – validation set

are based on the negligible difference of the R^2 statistic in calibration and validation when additional landscape data are added to the catchment area, implying no significant additional prediction input from these parameters. The results are summarised in Table 2.

What is evident from the table is that the one group of data is quite different from the other; Group 1 is stronger in calibration and validation than Group 2. The grouping was a random choice process and this result is probably due to the small sizes of the groups (respectively 13 and 12 stations). Larger data sets are probably required to eliminate the effects of outliers in the samples. Table 2 also shows that catchment area on its own is a sufficiently good predictor of floods and the addition of landscape data does not improve this by much. This observation is based on the values of R^2 for the validation group. Besides *Area*, when *Relief* and then *MAP* are included, the results are best for validation using Group 2 (0.556 and 0.553 respectively compared to 0.538 for *Area* only). Conversely, when Group 1 is used for validation, *Area* alone has

the best R^2 (0.856) followed by the inclusion of *Drainage Density* (0.784) and *MAP* (0.770). *Drainage Density* is an area surrogate, so the apparent strength in validation might be due to this fact, whereas MAP is independent of area.

Ultimately, designers require an efficient flood formula and the acquisition of landscape data is not easy nor does it seem to provide much help to use a more complicated formula. Thus the use of the RMF (area-based) empirical equations seems justified. However, since this is only a preliminary review, further investigations into the role of landscape in affecting a flood regime is required to help with the understanding of this phenomenon.

TABLE 2
Results of the step-wise regression

			R^2	
			Group 1: calib. Group 2: valid.	**Group 2: calib. Group 1: valid.**
Q_{20} vs..	Area	Calibration:	0.856	0.538
		Validation:	0.538 **(3)**	0.856 **(1)**
	Area and slope	Calibration:	0.869	0.566
		Validation:	0.534	0.724
	Area and MAP	Calibration:	0.886	0.552
		Validation:	0.507	0.770 **(3)**
	Area and drainage density	Calibration:	0.872	0.538
		Validation:	0.531	0.784 **(2)**
	Area and relief	Calibration:	0.875	0.644
		Validation:	0.556 **(1)**	0.628
	Area and ruggedness number	Calibration:	0.880	0.593
		Validation:	0.552	0.659
	Area, slope and MAP	Calibration:	0.896	0.635
		Validation:	0.502	0.393
	Area, ruggedness number and MAP	Calibration:	0.920	0.596
		Validation:	0.523	0.640
	Area, drainage density and MAP	Calibration:	0.887	0.571
		Validation:	0.488	0.534
	Area, relief and MAP	Calibration:	0.890	0.647
		Validation:	0.553 **(2)**	0.605

(1), (2) and **(3)**: These numbers in parentheses flag the "best" (based on the R^2 statistic) fit to the validation data.

Return period of the RMF

The RMF method of flood computation was applied to 57 catchments, where both annual flood peak data were available and where the regional *K*-values were known from Kovacs (1988). The floods were estimated for Regions 4.6, 5 and 5.2, which nearly cover the entire country (the remaining regions have a small number of recorded floods in their database). The floods were modelled from historical records using the GEV distribution and were plotted coaxially with those that were determined from the RMF, corresponding to the same regions and catchments, against catchment area as the independent variable as shown in Fig. 6. Since the return periods of the modelled floods were known, the return period of the RMF could then be estimated. For this reason, the 50-, 100- and 200-year floods were determined from the statistically modelled floods to determine the return period of the RMF. The results are shown in Figs. 6, 7 and 8 which cover Regions 4.6, 5 and 5.2 respectively.

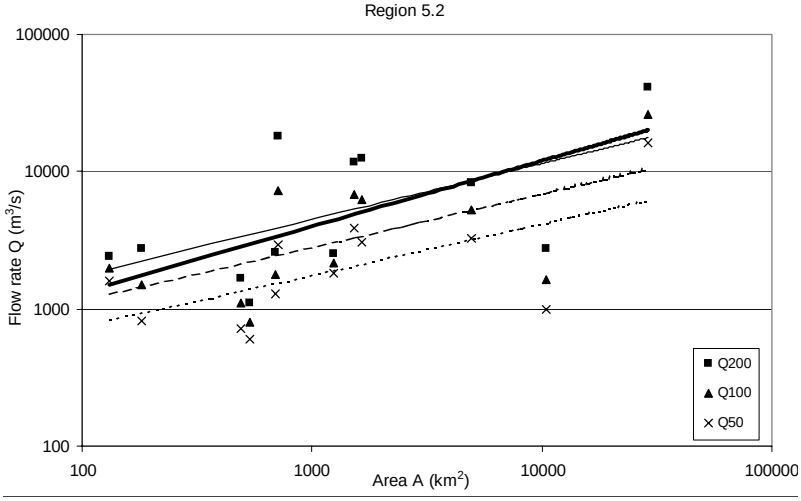

Figure 6
Determination of the return period associated with the RMF for Region 5.2. The bold line is the RMF estimate explained by the Francou-Rodier equation and the thin lines (dotted, dashed and solid) are trend-lines fitted to the 50-, 100-, and 200-year floods estimated from the recorded flows (points) in region 5.2, using the GEV distribution.

The 200-, 100- and 50-year observed flood magnitudes are represented by the thin solid line, the thin dashed line and the thin dotted line respectively. These magnitudes were determined from the statistical analysis of observed flood data for the individual catchments using the GEV distribution; a subset of the full data set (used for comparison with landscape analyses) appears in Part 3 of Table A1 in the **Appendix**. The RMF estimates were then determined from Kovacs (1988) using the Francou-Rodier equation and Kovacs' regional *K*-values for the corresponding catchments. These are represented by the thick solid lines in Figs. 6, 7 and 8. The 200-, 100- and 50-year flood estimates are plotted coaxially with the RMF estimates for the corresponding catchments in regions 4.6, 5 and 5.2 to examine if a return period can be associated with the RMF.

From Figs. 6, 7 and 8 it is clear that the RMF, when compared to the 50-, 100- and 200-year floods, is closest to the 200-year flood. The trend-line equations, summarised in Table 3, make for interesting reading. The slopes of the corresponding curves and

trend-lines are not equal. In fact the 200-, 100- and 50-year trend-line slopes are slightly flatter than the RMF curves for all the floods in all the regions except one (Q_{50} for Region 4.6); nevertheless, the correspondence is good and provides a starting point for further research to explain the similarities, even if the R^2 values are quite low.

In all three cases, the RMF line and the 200-year trend-line estimated from the fitted GEV distributions almost lie on top of each other and are very nearly parallel, mindful of the contents of Table 3. However, it must be admitted that the trend-lines for the 200-, 100- and 50-year floods have a poor fit and a fair amount of scatter can be observed. In all of Figs. 6, 7 and 8, serious outliers are evident for catchments with areas of about 1 000km², where the RMF is more likely to be associated with an event of return period of 100 years. On further investigation, it turns out that the problem 200-, 100-, and 50-year GEV flood estimate outliers are skewed by excessively large flood peaks that were observed in a relatively short record (between 20 and 30 years) for those catchments. It is expected that with more data, the effect of the outliers will be diminished. The result is that the plot for Region 5 (Fig. 7) is likely to be closer to the truth than Figs. 6 and 8 as it contains more data. In Fig. 7 the difference between the 200-year flood estimate and the RMF estimate is greater than the other two, but this difference is not excessive and the 200-year estimate and the RMF estimate are of the same magnitude. Based on these results, it is the opinion of the authors that it would be reasonable to assume the RMF to have a return period of the order of 200 years.

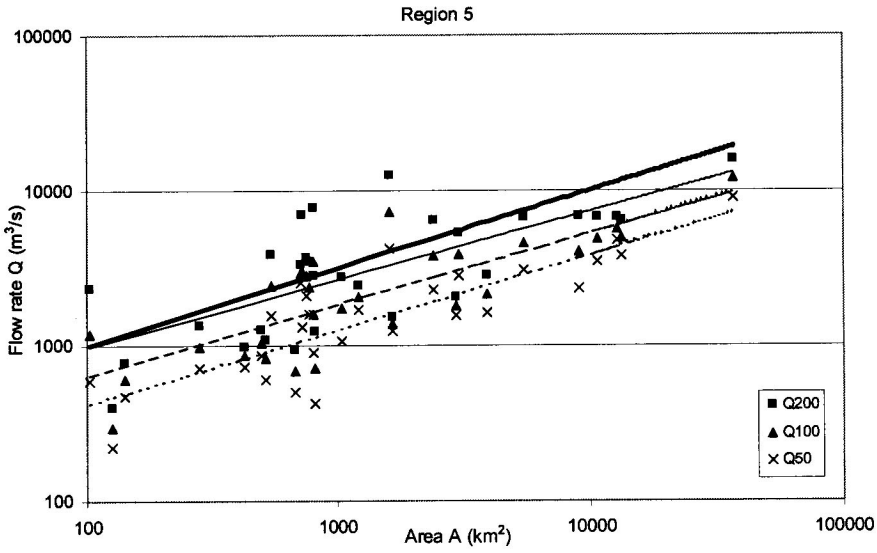

Figure 7
Determination of the return period associated with the RMF for Region 5 (description as per Fig. 6)

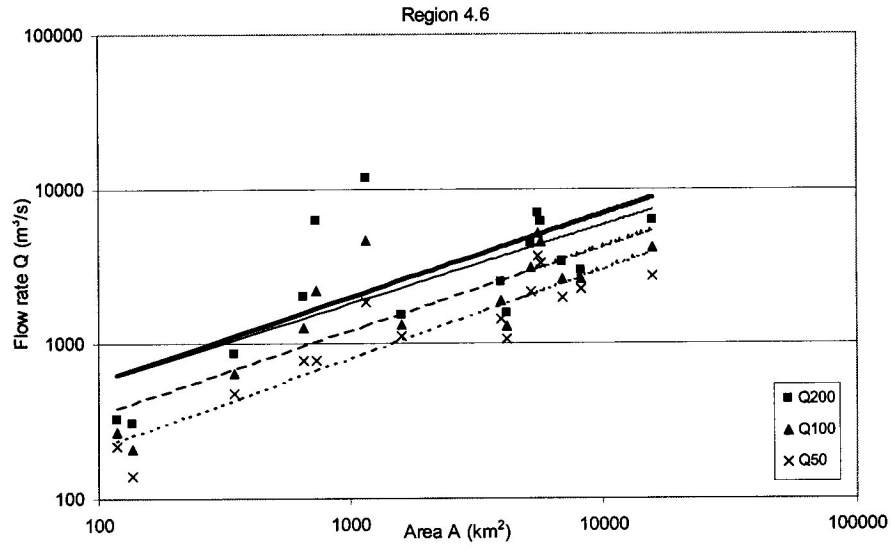

Figure 8
Determination of the return period associated with the RMF for Region 4.6 (description as per Fig. 6)

Q_T/Q_2 ratios in scaling floods

The Q_T/Q_2 ratios given in Table 1 are based on the premise that flood peaks in South Africa are log-normally distributed with a coefficient of variation equal to 1.3. To determine whether this average relationship is applicable in a design context, each of the maximum flood peaks recorded for the 130 catchments was assigned a return period based on the Weibull Plotting Position and then scaled down to 10- and 50-year events using the Q_T/Q_2 ratios. These flow rates were then plotted against the 10- and 50-year flow rates determined from modelling the historical records by the GEV distribution, to examine if the scaled flow rates are of the same order as the historical ones.

To simplify the analysis, a simple power-law relationship was sought between the ratios Q_T/Q_2 and T shown in Table 1. This short-cut approach was used instead of computing the percentage points of the lognormal distribution and to see its validity, the relationship is shown in Fig. 9, where a power law curve ($Q_T/Q_2 = 1.28T^{0.456}$) was fitted in the 10- to 100-year interval. This interval was used firstly because it fitted better ($R^2 = 0.996$) than a power-law curve through all the points and secondly, because all the recorded maxima were observed to lie in this interval, i.e. between 10 and 100 years. The plot of these scaled floods with the corre-

TABLE 3
Summary of the trend-lines from Figs. 6, 7 and 8

	Q_{RMF}	Q_{200}	Q_{100}	Q_{50}
Region 5.2	$145A^{0.48}$	$269A^{0.41}$	$191A^{0.39}$	$134A^{0.38}$
Region 5	$100A^{0.5}$	$129A^{0.44}$	$77A^{0.46}$	$45A^{0.48}$
Region 4.6	$48A^{0.54}$	$55A^{0.51}$	$29A^{0.54}$	$20A^{0.58}$

sponding 10- and 50-year floods modelled from historical records using the GEV distribution are shown in Figs 10 and 11.

Figure 10 indicates a reasonably good correspondence for the 10-year event between the GEV modelled flow rate and the scaled flow rate using the fixed lognormal distribution assumption. Fig. 11 indicates an excellent correspondence between the two estimates of flow rates for the 50-year event. The rarer floods are better estimated by the simple ratios than the more frequent ones because the 50-year flood is closer to the average of the record lengths. Even so, there seems to be little bias in the estimates, which might be useful if there is no distributional information. This will have to wait until a regional value of the GEV shape parameter k is obtained - this matter will be addressed below.

The modified rational formula (MRF)

Pegram (2003) introduced the concept of the MRF to enable the rational formula (RF) to be more efficient in flood prediction and more widely used for a variety of catchment sizes. He did this by replacing the rainfall intensity term (the i term in Eq. (5)) with a function that incorporates the median annual maximum rainfall, a scaling function of an extreme value distribution that includes the effect of return period and rainfall duration d. This last term is explicitly replaced by the time of concentration (using the Kirpich formula), which he showed is a function of catchment area, leading to the deduction that the areal reduction factors are nearly constant for a wide range of catchment sizes; the details can be found in Pegram (2003). The combination of these observations allows the MRF to be expressed as a simple function of the median annual maximum rainfall, the reduced variate of an extreme value distribution and catchment area as Eq. (7), repeated here:

$$Q_{MRF} = c \times 0.318 P_{1day,2} [1 + 0.385 y_T] A^{0.558} \quad (7)$$

The formula was introduced as a means of relating various scaling properties of the rainfall-runoff relationship to prompt discussion and further investigation, not as a serious design equation at this stage. Nevertheless, it was intriguing to determine how well it fared in comparison with the other methods described herein. 10-, 20- and 50-year floods based on the MRF were compared with the floods modelled by the GEV distribution from historical records. The values of c and $P_{1day,2}$ (refer to Eq. (7)) used here were based on Pegram's (2003) suggestions which were

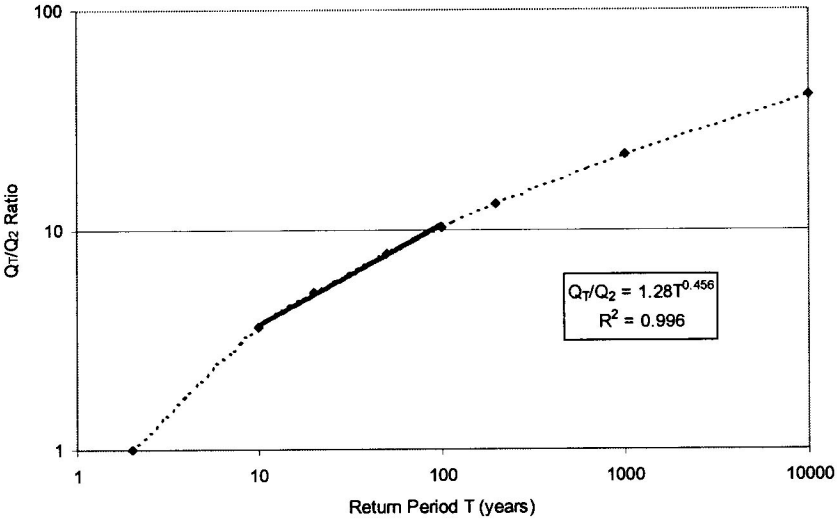

Figure 9
Plot of Q_T/Q_2 ratios vs. return period to determine a simple power-law relationship for the 10- to 100-year recurrence interval T

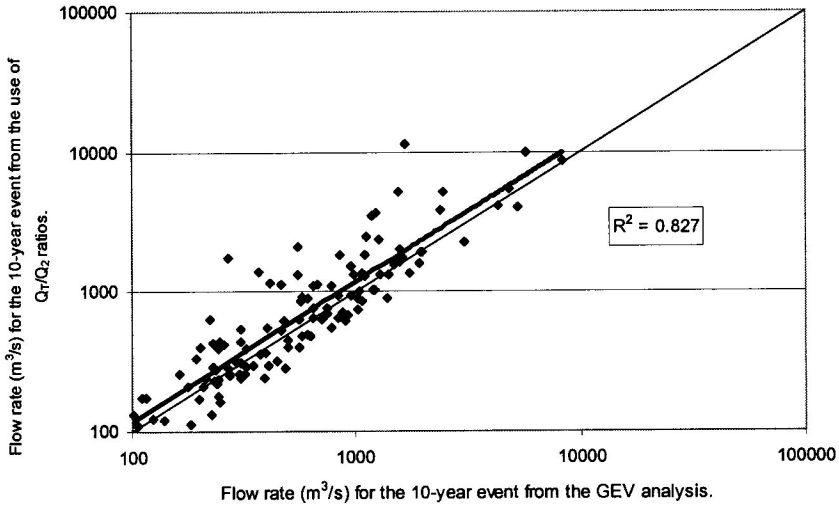

Figure 10
Comparison of Q_{10} flow rates using the Q_T/Q_2 ratios of Table 1 and Fig. 9, compared with those estimated from the GEV model fitted to the observed records

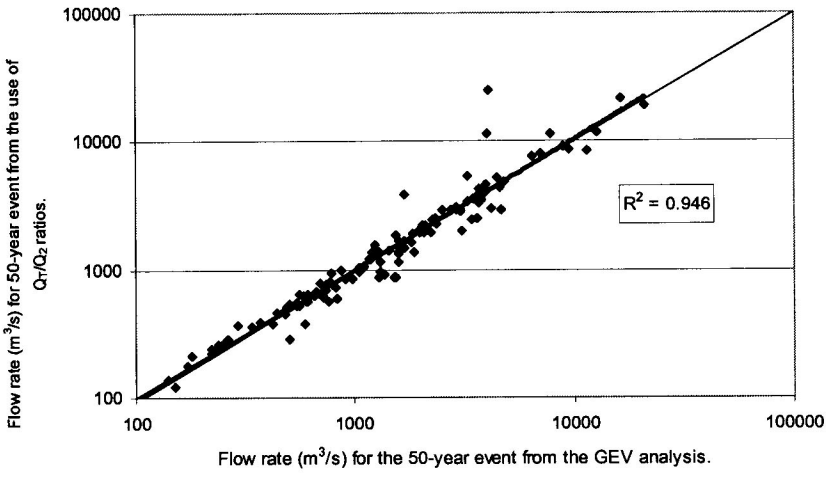

Figure 11
Comparison of Q_{50} flow rates using the Q_T/Q_2 ratios of Table 1 and Fig. 9, compared with those estimated from the GEV model fitted to the observed records

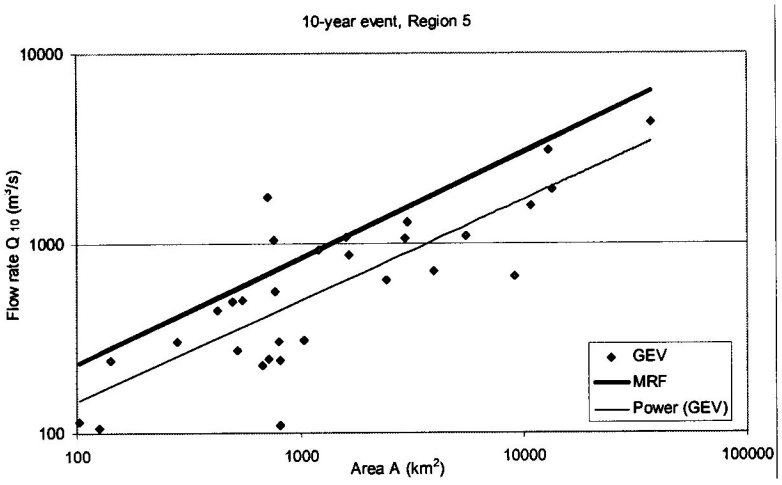

Figure 12

Comparison of the MRF, using $P_{1day,2}$= 60 mm for Region 5 and c=0.45 for the 10-year return period and the 10-year flood estimated from the GEV model fitted to the observed records

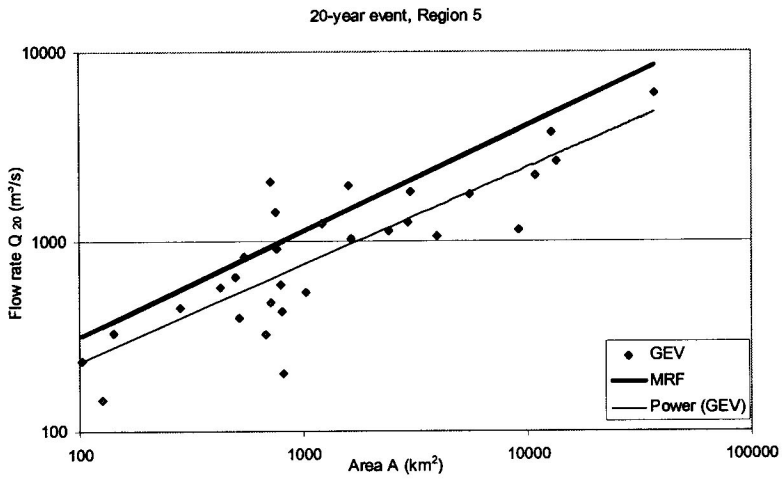

Figure 13

Comparison of the MRF, using $P_{1day,2}$= 60 mm for Region 5 and c=0.5 for the 20-year return period and the 20-year flood estimated from the GEV model fitted to the observed records

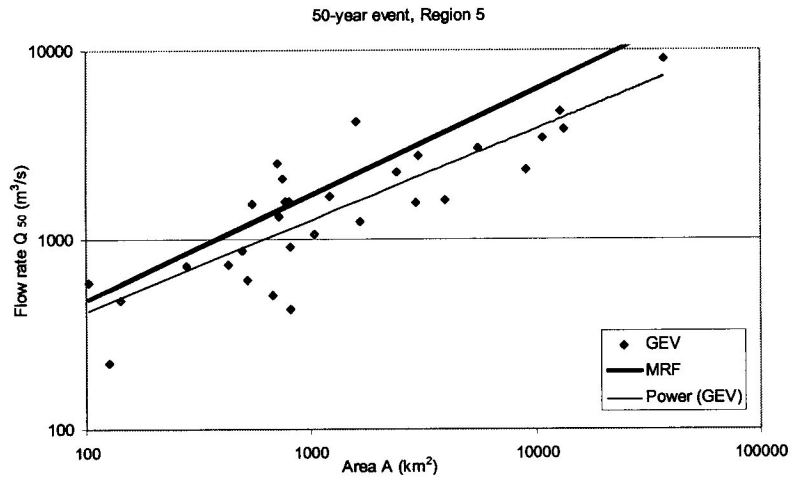

Figure 14

Comparison of the MRF, using $P_{1day,2}$= 60 mm for Region 5 and c=0.6 for the 50-year return period and the 50-year flood estimated from the GEV model fitted to the observed records

average values determined for each of Kovacs' *K*-regions. It is acknowledged that the values have as much as 25% variation within a region, depending on area, size and local conditions, however the aim of this preliminary study is to examine if the MRF's floods are of the same order as those observed and if this alternative is applicable. The regions used were Region 4.6, 5 and 5.2 and the $P_{1day,2}$ values were estimated as 45, 60 and 85mm respectively while values of 0.45, 0.5 and 0.6 were used for *c* for the 10-, 20 and 50-year events respectively. Values of $P_{1day,2}$ rainfall estimates for each Region *K* were determined by Pegram (2003) from Adamson's (1981) regional map of median annual maximum 1-day rainfall over South Africa. The value of *c* could vary from 0.45 to 0.75 (Pegram, 2003), which depends on soil type and land cover. With increasing recurrence interval, the role of rainfall abstractions becomes less as, during larger events, the catchment becomes more saturated and the vegetation gets stripped resulting in an increase in speed and volume of overland flow (AR&R, 2001). Mindfull of the fact that large to rare events such as the RMF are likely to have $T > 200$ years which would equate to a high value of *c*, and that the dominant land type is fairly flat grassland, the subjective estimates of *c*=0.45, 0.5 and 0.6 were made for the 10-, 20-, and 50-year return periods respectively.

The results of Region 5 (which covers the majority of the country) are shown in Figs. 12, 13 and 14. The results for the other two regions are very similar and the trend-line equations for all the regions are summarised in Table 4.

From Figs. 12, 13 and 14 and Table 4 it is evident that the MRF floods and those modelled with the GEV distribution are roughly of the same order of magnitude (although the 10-year GEV trend-line is over-estimated more than the 20- and 50-year events). The MRF floods are generally larger than the GEV floods for the same return period and this is true of all the regions. What is also evident is that the MRF floods model the GEV floods better as the return period increases (larger, less frequent events). This is also true of all the regions. In all figures, a large amount of scatter is observable in the plots of the GEV modelled historical flows. This is especially true for catchments of 1 000 km² area. As the recurrence intervals increase, the scatter becomes less and it would seem that the extreme value distribution is more suited to the 50-year recurrence interval floods.

The results indicate that the MRF computes floods of similar magnitude to those modelled, and the difference might be attributed to the choice of *c* and $P_{1day,2}$ values whose variation can be of the order of 25%, which Pegram (2003) suggests is probably twice the typical standard error associated with flood peak measurement. The conclusion is that the MRF provides a potential alternative "as a check formula for estimating flood peaks on a wide range of catchment areas for any recurrence interval" (Pegram, 2003). The discrepancy at smaller recur-

TABLE 4
Summary of the trend-line equations from Figs. 12, 13 and 14 for Region 5; and Regions 4.6 and 5.2 which are not shown.

	Region 5.2		Region 5		Region 4.6	
	MRF	GEV	MRF	GEV	MRF	GEV
Q_{10}	$25.2A^{0.558}$	$49.2A^{0.357}$	$17.8A^{0.558}$	$12.5A^{0.534}$	$13.3A^{0.558}$	$2.51A^{0.679}$
Q_{20}	$34.0A^{0.558}$	$79.6A^{0.359}$	$24.0A^{0.558}$	$22.1A^{0.511}$	$18.0A^{0.558}$	$5.78A^{0.630}$
Q_{50}	$81.7A^{0.558}$	$133.6A^{0.374}$	$36.5A^{0.558}$	$45.5A^{0.482}$	$27.4A^{0.558}$	$15.0A^{0.577}$

TABLE 5
Statistics of the GEV *k* and Kovacs' regional *K*

Kovacs *K*	Mean GEV *k*	Standard Error
5.2	-0.671	0.102
5	-0.477	0.0585
4.6	-0.463	0.113

rence intervals might be attributable to several sources - the choice of coefficients *c* based on return periods only rather than including more detailed considerations of land type and cover, the use of the median instead of the 10- or 20-year rainfall (also available from maps (Adamson, 1981)), the GEV shape parameters of the rainfall, chosen as a fixed $k = -0.18$, which is far less skew than streamflow which averages $k = -0.5$ (see below). What is encouraging is that the slopes of the lines are not that different. For larger events, the MRF flood estimates are closer to the GEV modelled floods.

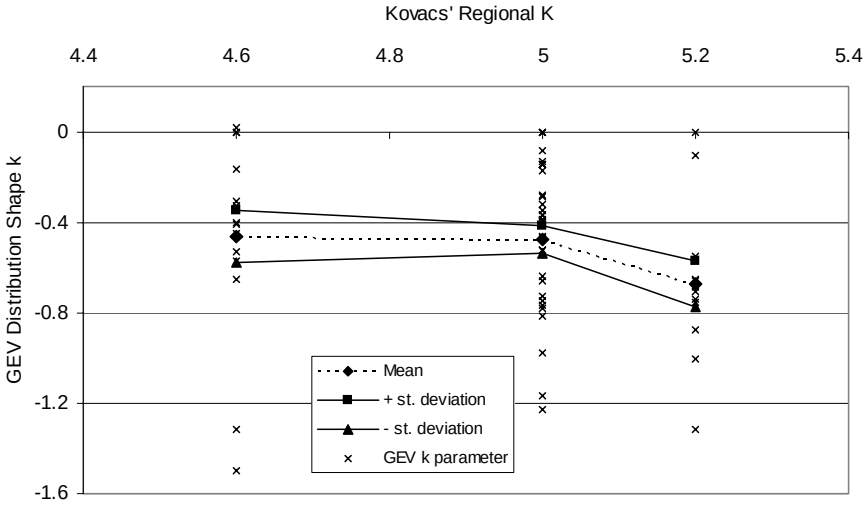

Figure 15
Plot of GEV k *(shape parameter) and* mean *plus and minus a standard deviation, vs. Kovacs' regional* K*-value for Regions 4.6, 5 and 5.2*

Regional GEV distribution values

The parameters of the GEV distribution include a shape parameter *k*. The relationship between this value and the regional *K*-value introduced by Kovacs (1988) is now examined to detect if any trend exists. The GEV *k* was allowed to assume any fitted value above -1.5. The lower limit was placed on the distribution in cases where extreme outliers skewed the extrapolation to unreasonable flood magnitudes. The GEV *k*, because it was determined by minimising the least squares in the model, was hoped to display a trend with the regional *K*-values. The GEV *k* and the regional *K* were plotted against each other for Regions 4.6, 5 and 5.2. The results are summarised in Table 5 and are shown in Fig. 15.

From Fig. 15, it is evident from the mean that no strong relationship exists. The GEV *k*-value for each catchment is plotted against the regional *K*-value for the region in which it is found. The mean GEV *k* for each region, plus and minus a standard deviation, are also plotted and show that the least deviation is for Region 5, where most of the data are. However, no real conclusion can be attributed to only three points and the lack of catalogued regional *K*-values for many of the catchments possibly account for this shortfall. The results are inconclusive; however, it would be nice to think that a relationship did exist (as shown by Kjeldsen et al., 2002) and that the modelling of historical floods could be regionalised, perhaps using some regional definition other than the RMF.

Conclusion

It is difficult to place exact values on flood magnitudes and their probabilities of occurring. No one method (empirical, deterministic and probabilistic) can be accepted *a priori* as better than the other, as all methods are approximations and their accuracy is relative. However, if one has a sufficiently long period of record, then one can make reasonably accurate predictions on future floods based on what was observed in the past. This premise is based on the assumption that climatic and geological controls in flood production remain the same as when the floods were observed. The database of annual flood peaks for the 130 catchments around South Africa allowed us to utilise the probabilistic method in determining future flood magnitudes that were, in all probability, representative of the truth. This database was used as a reference set to validate the other methods in review.

The addition of landscape data in an attempt to improve flood prediction was not particularly dramatic, nor did it provide much insight into which geomorphometric controls are involved in flood response. The role of landscape in flood production is not in doubt; however, further investigation is required in this regard. Larger sets of landscape data at accurate scales are required to assist in this endeavour. In this preliminary study it was found that landscape data do not make flood prediction more accurate and the area-based RMF empirical equation seems best. If an understanding of the role of landscape in flood production is required then the study should perhaps be based on physical and scaling, rather than statistical relationships.

The RMF method of flood computation is a versatile and easy method to compute the upper limit of floods that a site or region has historically experienced within the observed period of record. In this paper it was found that the return period of the RMF is approximately 200 years and this will no doubt increase the popularity of this method. If the return period is known, the RMF

can now be used as a convenient check method to ascertain the validity of design flood magnitudes. Once the data set used in this paper is augmented by 15 or more years of observed annual floods, refinements are likely to appear.

The use of the Q_T/Q_2 ratios, suggested in TRH 25 (1994), was found to scale observed flood maxima to flow rates with desired return periods reasonably accurately. The Weibull Plotting Position was used to associate a return period with the flood maxima and was based on the flood having been observed within the 10- to 100-year interval. The floods were reduced to 10- and 50-year flow rates through interpolation of the ratios; extrapolation to larger events is yet to be tested.

The use of the MRF proved to be a useful modification of the conventional rational formula and predicted flood magnitudes of similar order to those observed. It has potential to provide an alternative to other flood computation methods and might be used as a check formula for design floods for a wide variety of catchment sizes and return periods, especially where site-specific rainfall data and *c*-values are used.

The GEV scaling parameter *k* did not show any particular trend with the regional *K*-values. Other definitions of regionalisation may allow a stronger relationship; it is known that more arid areas experience floods with higher skew which in turn should give more negatively biased *k*-values. Our results were inconclusive, but again, more observed flood data should refine this.

The thoughts and ideas presented in this paper are here to serve as preliminary insight into some interesting relationships between some of the flood determination methods employed in South Africa. Admittedly, the flood database used in this investigation is 15 years old, and in many instances, a fair degree of scatter is observable in the flood distributions. Longer records of floods are required to possibly eliminate these anomalies. However, the flood database utilised did provide a consistent foundation to launch this review.

References

ADAMSON PT (1981) Southern African Storm Rainfall. Tech Rep TR102. Dept. Environ. Affairs, Div. Hydrology, Pretoria.

ALEXANDER WJR (2002) The Standard Design Flood – Theory and Practice. Dept of Civil Engineering, University of Pretoria, Pretoria.

AUSTRALIAN RAINFALL AND RUNOFF (2001) *A Guide to Flood Estimation*. Pilgrim DH (editor-in-chief). The Institution of Engineers, Australia.

DE MICHELE C and SALVADORI G (2002) On the derived flood frequency distribution: analytical formulation and the influence of antecedent soil moisture condition. *J. Hydrol.* **262** (1-4) 245-258.

FSR (1975) *Flood Studies Report. **Vol. 2** Meteorological Studies*. Natural Environment Research Council, London.

HIEMSTRA LAV and FRANCIS DM (1979) The Runhydrograph – Theory and Application for Flood Predictions. Water Research Commission, Pretoria.

HORTON RE (1932) Drainage basin characteristics. *Trans. Am. Geophys. Union.* **13** 350-361.

HORTON RE (1945) Erosional development of streams and their drainage basins: Hydrophysical approach to quantitative morphology. *Bull. Geol. Soc. Am.* **56** 275-370.

KJELDSEN TR SMITHERS JC and SCHULZE RE (2002) Regional flood frequency analysis in the KwaZulu-Natal Province, South Africa, using the index-flood method. *J. Hydrol.* **255** (1-4) 194-211.

KIRPICH ZP (1940) Time of concentration of small agricultural watersheds. *Civ. Eng.* **10** (6) 362.

KOVACS Z (1988) Regional Maximum Flood Peaks in Southern Africa. Technical Report TR 137, Department of Water Affairs, Pretoria.

MIDGLEY DC, PITMAN WV and MIDDLETON BJ (1994) Surface Water Resources of South Africa, 1990. WRC Report No. 298/1/94.

PARAK M (2003) The Flood-Landscape Relationship. Unpublished undergraduate dissertation. School of Civil Engineering, University of KwaZulu-Natal, Durban.

PEGRAM GGS (2003) Rainfall, rational formula and regional maximum flood – Some scaling links. Keynote Paper. *Aust. J. Water Resour.* **7** (1) 29-39.

PETRAS V and DU PLESSIS PH (1987) Catalogue of Hydrological Parameters. Flood Studies. Technical Note No. 6, Department of Water Affairs, Pretoria.

SHREVE RL (1966) Statistical law of stream numbers. *J. Geol.* **74** 17-37.

SMITHERS JC and SCHULZE RE (2003) Design Rainfall and Flood Estimation in South Africa. WRC Report 1060/1/03, Water Research Commission, South Africa.

STRAHLER AN (1952) Hypsometric (area-altitude) analysis of erosional topography. *Bull. Geol. Soc. Am.* **63** 1117-1142.

STRAHLER AN (1964) Quantitative geomorphology of drainage basins and channel networks. In: VT Chow (ed.) *Handbook of Applied Hydrology*. Sec. 4-11. Mcgraw Hill, New York.

TRH 25 (1994) *Guidelines for the Hydraulic Design and Maintenance of River Crossings.* **Vol. 1** 2-21 *Hydraulics, Hydrology and Ecology*. Pretoria, Department of Transport.

WESTRAY L (2001) Linking Rational Formula to the Regional Maximum Flood formula to give the Modified Rational Formula (MRF). Unpublished undergraduate dissertation. School of Civil Engineering, University of KwaZuluNatal, Durban.

Appendix

Hydrologic and morphometric parameter definitions (from Parak, 2003):

1. Catchment area: A (km²)

This is the gross catchment area that is represented by the relevant gauging station.

2. Ineffective area: A_{in} (km²)

This includes those areas from which runoff cannot reach the river, for example from pans or depressions.

3. Effective area: A_e (km²)

This is the part of the catchment area that contributes runoff to the rivers and ultimately the relevant gauging station. It is the difference between the gross catchment area and the ineffective area.

4. Catchment perimeter: P (km)

This is the distance measured along the catchment boundary, i.e. the distance along the watershed boundry.

5. Longest water course: L (km)

This is the distance from the gauging station along the longest watercourse to furthest point on the channel, i.e the start of the permenent streams (fingertip tributary) near the catchment boundary.

6. Maximum elevation above sea level: Z_m (m)

This is the point of maximum height above sea level on the catchment divide (watershed).

7. Elevation of gauging station above sea level: Z_o (m)
This is the elevation of the gauging station above sea level.

8. Catchment relief: R (m)
This is defined as the height difference between the maximum elevation on the watershed and the elevation of the gauging station. It is thus the difference between Z_m and Z_o.

9. Mean river slope: S
The mean slope of the channel or river is computed from the longitudinal profile of the river along the main watercourse from the furthest point along the channel (fingertip tributary) by equating the cut and fill areas (refer to Fig. A1).

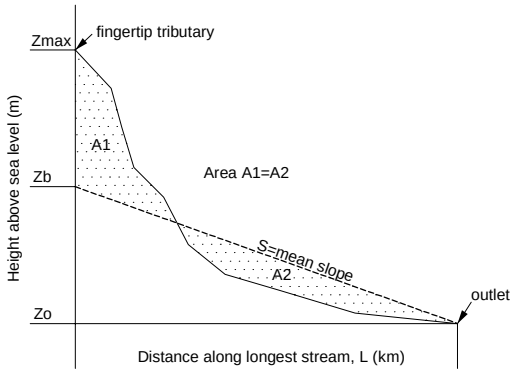

Figure A1
The mean channel slope (after Petras and Du Plessis, 1987)

10. Shape factor: A/A_c
This is the ratio of the gross catchment area (A) to the area of a circle (A_c) drawn from the longest possible catchment diagonal (refer to Fig. A2).

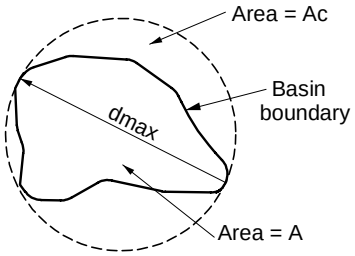

Figure A2
The shape factor A/A_c (after Petras and Du Plessis, 1987)

11. Time of concentration: T_c (hours)
This is the time required for a water particle to travel from the catchment boundary along the longest watercourse (L) to the gauge at the basin outlet, and was computed from Kirpich (1940):

$$T_c = 0.0633\left(\frac{L}{S}\right)^{0.385} \qquad \text{(A1)}$$

12. Mean annual precipitation: MAP (mm)
This was determined on 1:250000 scale isohyetal maps.

13. Mean annual runoff: MAR (10^6 m^3)
This was obtained from the gauging records.

14. Maximum observed flood peak: Q_{max} (m^3/s)
These are the maximum observed flood peaks recorded at the relevant stations for the length of the representative period.

15. Representative period: N (years)
This is not the return period, but the length of record at the gauges.

16. RMF K-value of region
This is the K-value of the region where the gauging station is found, determined from the Map of Maximum Flood Peak Regions in Southern Africa (Kovacs, 1988). This map devides South Africa into hydrologically homogeneous regions.

17. Total length of all streams in basin: ΣL (km)
This is the sum of the lengths of all the streams and channels which feed the catchment outlet at the gauge. This was determined from a 1:250000-scale map.

18. Strahler basin order
This is the order of the channel, ordered according to the method of Strahler (1952), at the catchment outlet (see Fig. A3(a)). The smallest recognisable channels (fingertip tributaries) are designated order *1*. Where two channels of order *i* join, a channel of order *i+1* forms downstream. Where a channel of order *i* and *i+1* join, the channel downstream assumes the order of the higher channel. These were determined from 1:250000-scale maps.

19. Shreve magnitude
This is the order of the channel, ordered according to the method of Shreve (1966), at the catchment outlet (see Fig. A3(b)). The Shreve magnitude of a catchment stream network reflects the number of fingertip tributaries feeding the catchment outlet. At the junction of two streams, the resulting order of the downstream channel is the sum of the orders of the two streams feeding it. These were determined from 1:250000-scale maps.

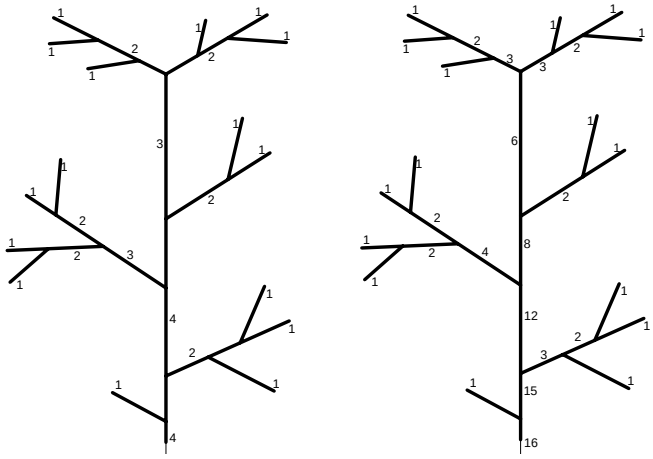

Figure A3
Two methods of stream ordering
(a) Strahler basin order
(b) Shreve magnitude

20. Drainage density DD (km/km^2)
This is the quotient of total stream length within a catchment and the catchment area, determined by dividing ΣL by A.

21. Ruggedness number RN
This is defined as the product of drainage density and catchment relief, i.e. *RN=DDxR.*

22. Bifurcation Ratio R_b
This was determined by plotting the number of streams in each order of a catchment on a logarithmic scale with the stream order on a linear scale. The slope of the fitted regression line is the bifurcation ratio.

TABLE A1
Hydrological and morphometric data for those catchments in South Africa whose data overlapped/intersected (Part 1)

Gauge number	River	Petras and Du Plessis (1987)										
		Catchment area (km^2)	Ineffective area (km^2)	Effective area (km^2)	Catchment perimeter (km)	Longest water course (km)	Catchment relief (m)	Mean river slope	Shape Factor A/A_c	Time ofconc. (hours)	Mean annual precipi-tation (mm)	Mean annual runoff (x 10^6 m^3)
A2H003	HEX	495	6	489	103.0	36.0	616	0.00917	0.49	6.4	705	15.0
A2H004	PLAT	137	0	137	57.0	22.0	480	0.01320	0.68	3.8	698	7.5
A2H007	APIES	142	0	142	51.0	16.0	289	0.01220	0.42	3.1	770	3.6
B1H001	OLIFANTS	3 989	0	3 989	263.0	172.0	395	0.00155	0.66	42.0	700	127.0
B2H001	BRONKHORST	1 594	0	1 594	183.0	78.3	308	0.00288	0.39	18.1	700	50.0
C1H002	KLIP	4 152	0	4 152	330.0	181.0	820	0.00132	0.56	47.0	785	325.0
C4H001	GROOT VET	5 590	0	5 590	350.0	127.0	645	0.00151	0.72	34.0	218	218.0
C5H007	RENOSTER	348	0	348	94.0	39.8	305	0.00332	0.37	10.2	550	8.7
C6H001	VALS	5 674	50	5 624	414.0	260.0	940	0.00119	0.29	64.0	629	209.0
C8H001	WILGE	15 673	0	15 673	530.0	377.0	1 790	0.00047	0.66	122.0	756	717.0
D1H001	WONDER	2 397	0	2 397	233.0	99.4	831	0.00362	0.52	19.9	488	48.0
H1H006	BREE	753	0	753	132.0	50.0	1 768	0.01130	0.66	7.6	1 040	271.0
H2H003	HEX	718	0	718	152.0	60.8	1 966	0.01130	0.43	8.8	939	162.0
L1H001	SOUT	3 938	0	3 938	270.0	124.0	945	0.00397	0.65	23.0	222	26.0
N3H001	VOEL	1 597	0	1 597	195.0	129.0	1 717	0.00485	0.32	22.0	368	39.0
Q1H001	GROOT VIS	9 091	10	9 081	474.0	107.0	1 449	0.00545	0.51	18.0	370	950.0
Q6H001	BAVIAANS	694	0	694	128.0	59.5	1 254	0.01067	0.49	8.9	620	22.0
R2H005	BUFFALLO	411	0	411	100.0	45.0	939	0.00635	0.57	8.7	880	43.0
S3H002	KLAAS SMITS	796	0	796	141.0	52.0	883	0.00660	0.62	9.6	505	21.0
T3H004	MZIMHLAVA	1 029	0	1 029	157.0	98.0	1 027	0.00411	0.32	18.8	885	106.0
T5H004	MZIMKULU	545	0	545	109.0	42.5	1 832	0.13640	0.55	6.2	1 200	236.0
V3H005	SLANG	676	0	676	125.0	73.8	594	0.00335	0.60	16.4	955	139.0
V6H002	TUGELA	12 862	0	12 862	492.0	297.0	2 571	0.00318	0.65	48.0	920	2 946.0
W5H006	SWARTWATER	180	0	180	60.5	29.0	469	0.01096	0.61	5.0	955	35.0
X1H001	KOMATI	5 499	0	5 499	378.0	207.0	1 092	0.00504	0.48	31.0	890	623.0

ISSN 0378-4738 = Water SA Vol. 30 No. 3 July 2004

TABLE A1
Hydrological and morphometric data for those catchments in South Africa whose data overlapped/intersected (Part 2)

Gauge number	River	Kovacs (1988)				Extracted from Midgley et al. (1994)					
		Max obs. flood peak (m^3/s)	Repre-sent. period (years)	Regio-nal K-value	Q_{RMF} (m^3/s)	Total stream length (km)	Strahler order	Shreve magni-tude	Drainaged ensity (km/km^2)	Rugged-ness number	Bifur-cation ratio
A2H003	HEX	709	25	5	2 225	144.9	3	12	0.296	0.183	1.55
A2H004	PLAT	126	37	4.6	682	46.8	2	2	0.342	0.164	2
A2H007	APIES	454	79	5	1 192	24.1	2	2	0.169	0.49	2
B1H001	OLIFANTS	1 330	47	4.6	4 212	1 003.2	5	53	0.251	0.0993	1.62
B2H001	BRONKHORST	1 030	47	4.6	2 567	352.0	3	21	0.221	0.068	1.62
C1H002	KLIP	1 220	69	4.6	4 304	1 286.7	4	96	0.31	0.254	2.1
C4H001	GROOT VET	4 380	65	4.5	5 054	1 608.0	4	129	0.288	0.186	1.82
C5H007	RENOSTER	800	65	4.6	1 128	99.0	2	9	0.284	0.0868	1.29
C6H001	VALS	2 560	75	4.6	5 094	1 422.4	4	91	0.253	0.238	1.57
C8H001	WILGE	3 120	74	4.6	8 818	5 243.0	5	415	0.335	0.599	1.86
D1H001	WONDER	2 690	76	5	4 896	349.1	2	2	0.146	0.121	2
H1H006	BREE	1 140	66	5	2 744	317.1	3	33	0.421	0.745	2.03
H2H003	HEX	737	38	5	2 680	346.5	4	41	0.483	0.949	2.03
L1H001	SOUT	2 240	55	5	6 275	1 133.7	5	74	0.288	0.272	1.79
N3H001	VOEL	1 980	19	5	3 996	530.5	4	37	0.332	0.57	1.48
Q1H001	GROOT VIS	2 640	70	5	9 535	1 940.4	5	117	0.214	0.31	2.56
Q6H001	BAVIAANS	895	19	5.2	3 341	99.8	2	7	0.144	0.18	1.4
R2H005	BUFFALLO	1 050	41	5.4	3 329	84.7	2	3	0.206	0.194	1.5
S3H002	KLAAS SMITS	906	25	5	2 821	73.7	2	2	0.0926	0.0818	2
T3H004	MZIMHLAVA	759	41	5	3 208	435.0	4	47	0.423	0.434	2.01
T5H004	MZIMKULU	651	39	5	2 335	274.6	3	35	0.504	0.923	1.64
V3H005	SLANG	400	33	5	2 600	251.4	3	25	0.372	0.221	2.04
V6H002	TUGELA	4 610	41	4	11 341	5 143.5	6	486	0.4	1.028	1.92
W5H006	SWARTWATER	600	37	5.2	1 748	71.5	3	8	0.397	0.186	2
X1H001	KOMATI	3 420	49	5	7 416	1 697.1	4	118	0.309	0.337	1.52

TABLE A1
Hydrological and morphometric data for those catchments in South Africa whose data overlapped/intersected (Part 3)

Gauge number	River	GEV modelled flow rates from recorded flood data								Flow rates scaled by Q_T/Q_2 ratios in Table 1	
		Length of record (years)	Q_2(m³/s)	Q_{10}(m³/s)	Q_{20}(m³/s)	Q_{50}(m³/s)	Q_{100}(m³/s)	Q_{200}(m³/s)	Shape parameter k	Q_{10}(m³/s)	Q_{50}(m³/s)
A2H003	HEX	24	185	499	648	869	1 060	1 273	-0.1692	446	976
A2H004	PLAT	42	9	49	79	140	209	309	-0.5301	67	146
A2H007	APIES	46	78	241	330	476	613	780	-0.2816	171	374
B1H001	OLIFANTS	45	127	651	945	1 437	1 908	2 490	-0.3057	633	1 384
B2H001	BRONKHORST	47	20	608	829	1 111	1 320	1 527	0.0140	490	1 072
C1H002	KLIP	71	164	578	774	1 063	1 310	1 586	-0.1628	489	1 069
C4H001	GROOT VET	24	447	1 619	2 361	3 704	5 100	6 942	-0.4037	1 804	3 940
C5H007	RENOSTER	38	36	207	308	480	651	866	-0.3407	329	720
C6H001	VALS	61	495	1 494	2 129	3 284	4 488	6 081	-0.4081	988	2 160
C8H001	WILGE	60	233	974	1 546	2 736	4 149	6 243	-0.5705	1 212	2 648
D1H001	WONDER	65	123	643	1 123	2 265	3 802	6 344	-0.7280	1 032	2 256
H1H006	BREE	28	401	1 041	1 429	2 111	2 801	3 688	-0.3684	466	1 019
H2H003	HEX	28	101	248	479	1 321	2 997	6 925	-1.2274	386	843
L1H001	SOUT	41	92	717	1 060	1 624	2 157	2 805	-0.2865	994	2 172
N3H001	VOEL	20	145	1 077	1 976	4 189	7 263	12 491	-0.7680	1 405	3 071
Q1H001	GROOT VIS	58	187	671	1 146	2 331	3 995	6 858	-0.7832	1 051	2 297
Q6H001	BAVIAANS	19	498	710	890	1 290	1 797	2 591	-0.6509	635	1 388
R2H005	BUFFALLO	26	392	832	1 001	1 218	1 382	1 544	-0.0001	531	1 161
S3H002	KLAAS SMITS	29	111	306	594	1 590	3 477	7 711	-1.1648	571	1 247
T3H004	MZIMHLAVA	30	36	309	541	1 062	1 726	2 772	-0.6588	384	839
T5H004	MZIMKULU	28	106	500	829	1 552	2 456	3 860	-0.6364	337	736
V3H005	SLANG	34	72	228	327	507	693	940	-0.4053	223	487
V6H002	TUGELA	45	1 563	3 071	3 767	4 787	5 649	6 601	-0.1484	2 333	5 097
W5H006	SWARTWATER	33	37	193	363	821	1 511	2 777	-0.8742	318	694
X1H001	KOMATI	76	205	1 104	1 758	3 066	4 558	6 695	-0.5213	1 598	3 492